Tribology Online

Japanese Society of Tribologists
https://www.tribology.jp/trol/

Vol. 18, No. 5 (2023) 217-231.
ISSN 1881-2198
DOI 10.2474/trol.18.217

Article

Comparison of the Sliding Behavior of Several Polymers in Gaseous and Liquid Hydrogen

Géraldine Theiler* and Thomas Gradt

Bundesanstalt für Materialforschung und -prüfung (BAM), 12200 Berlin, Germany

*Corresponding author: Géraldine Theiler (geraldine.theiler@bam.de)

Manuscript received 27 February 2023; accepted 22 June 2023; published 31 August 2023
Presented at the 7th World Tribology Congress 2022 Lyon, July 2022

Abstract

The development of hydrogen technologies entails high safety requirements in distribution and dispensing infrastructure. Therefore, it is necessary to pursue research on material compatibility in hydrogen, especially for critical parts with tribological issues. The focus of this study is to evaluate the influence of hydrogen on a wider range of commercially available polymer materials. Thereby, the friction and wear behavior of different grades of TPE, POM, PA66, PA12, PPA, PEEK, PPS, PTFE, PAI, PI and PBI were investigated against a rotating steel disk (AISI 304). Filled and unfilled polymers from different suppliers were evaluated at room temperature in air, vacuum and hydrogen gas (H_2) as well as in liquid hydrogen at -253°C (LH_2). The sliding behavior of the polymer materials is discussed by means of surface analyses, whereby special attention is paid to the formation of a transfer film. According to the results at ambient temperature, the effect of hydrogen environment on the tribological behavior of neat polymers may be related to lack of moisture, but also to saturated hydrocarbons in gaseous hydrogen. In liquid hydrogen, the best tribological performances were achieved with neat PA polymers as well as PPS and PI composites.

Keywords

polymers, composites, sliding wear, hydrogen, cryogenic temperature

1 Introduction

To enable decarbonization, new national strategies aim to establish hydrogen as an alternative energy carrier and to enhance its use in transport and industry. The development of hydrogen technologies entails high safety requirements in distribution and dispensing infrastructure. Many critical parts contain tribosystems, examples are joints, compressors and valves. As sealing components, polymeric materials are used in a wide range of applications e.g. as O-rings and piston rings in high-pressure and/or cryogenic hydrogen. As it is well known that the environment is an important issue on the tribological behavior of polymer materials, research on material compatibility in hydrogen is crucial for safety and reliability purpose.

The compatibility of polymer materials for hydrogen applications has been the focus of investigations since many years [1-8], but only few publications on the friction behavior of polymers are availble [9-18]. Up to now, few studies have been published on the reciprocating behavior of rubber materials [9-11], while the sliding performance of PTFE based materials in high-pressure hydrogen up to 40 MPa has been deeply investigated by Sawae [12-15]. Special attention was taken to tribochemical reactions, transfer film formation, and relative humidity in hydrogen. Authors' previous works on the sliding performances of PEEK and PI materials in hydrogen at normal pressure pointed out the effect of polymer structure, fillers, sliding velocity, temperature and counterface material in hydrogen environment [16-18].

Besides a technical note from NASA, published in the 1960 [19], reports on the friction behavior of polymers in LH_2 are scarce [20-24]. While the effect of the cryogenic medium was reported in [20, 21], tribochemical reactions could be detected with PTFE materials down to 20 K. Further tribological tests in LH_2 performed with several composites against 52100 indicated the effect of the fillers, cryogenic medium or velocity [22-24].

The purpose of this study is to evaluate the sliding performance of a wide range of commercially available polymer materials in gaseous and liquid hydrogen. In a first stage, the aim is to identify the effect of hydrogen environment on the tribological behavior of neat polymers and composites sliding against 304 stainless steel by comparing with air and vacuum at ambient temperature. The second part deals with the sliding performance of these polymer materials in liquid hydrogen by comparing with gaseous hydrogen at ambient condition to study the effect of low temperature only.

2 Experimental details

2.1 Materials

A wide range of commercially available materials were chosen based on the following polymers: Thermoplastic elastomer (TPE), Polyoxymethylene (POM), Polyamides (PA66, PA12), Polyphenylene sulfide (PPS), Polytetrafluoroethylene (PTFE), Polyether ether ketone (PEEK), Polyphthalamide (PPA), Polyamide-imide (PAI), Polyimides (PI1, PI3) and Polybenzimidazoles (PBI). In addition, different grades of PA, PEEK and PI from different suppliers, chemistry or molecular weight were included in this study. Composite materials contain conventional solid lubricants like graphite (Gr), PTFE (in the composites referred as TF) and MoS_2, and further fillers and fibers such as carbon fibers (CF), milled glass fibers (GF) or bronze (Br). Comparing to our previous works with PEEK and PI materials [16-18], only neat PI1 was used in this study. Table 1 summaries the 25 materials evaluated.

2.2 Experimental setup

Tribological tests were performed in the CT2 tribometer developed at BAM and described in detail in [25]. It is thermally insulated by vacuum superinsulation and cooled directly by a bath of liquid cryogen. Loading is performed by means of a gas bellows which acts on a frame with the fixed sample (pin) mounted on its lower beam. The rotating journal is sealed by a ferrofluidic rotary feedthrough at the top flange of the cryostat. The friction force is measured by means of a torque sensor on top of the motor journal. Experiments were conducted at room temperature in air (moisture range 40%-60%), in hydrogen gas (H_2) at 10^5 Pa (H_2O < 5ppm) and in high vacuum at 10^{-3} Pa. Cryogenic tests were performed in liquid hydrogen (LH_2) (-253°C, H_2O < 5ppm). Before testing in H_2, the tribometer was evacuated to 10^{-3} Pa. For LH_2 tests, the cryogenic chamber was additionally purged with helium.

The samples were arranged in a pin-on-disk configuration with a flat pin continuously sliding against a rotating disk. The counterpart was an austenitic stainless steel (AISI 304) with a ground surface roughness of Ra = 0.2 μm and an outside diameter of 60 mm. All sliding tests were performed under dry conditions with an average contact pressure of 3.1 MPa and a sliding speed of 0.2 m/s.

The wear of the polymer composites was determined by measuring the weight loss of the worn pin minus the weight loss of a reference pin placed inside the tribometer. This method was used to consider any weight changes of the polymer pin due to vacuum pumping or hydrogen uptake during the test. The weight loss was measured after 5000 m sliding in air and hydrogen at ambient temperature and after 3000 m sliding in liquid hydrogen.

The specific wear rate was calculated by using Eq. (1).

$$W_s = \frac{\Delta m}{\rho \times F_N \times L} \left[\frac{mm^3}{N \times m}\right] \quad (1)$$

Where Δm is the mass loss of the worn sample during the test minus weight loss of the reference sample, ρ is the density, F_N the applied normal force and L the total sliding distance.

Several repeats were done per material and test condition (two in LH_2 and up to four at ambient temperature). The friction force was recorded during the test and the average friction coefficient is the mean value of repeats obtained at the end of the tests (5000 m at ambient temperature, 3000 m in LH_2).

Table 1 Materials evaluated

POLYMERS		COMPOSITES
TPE		
POM		
PA66	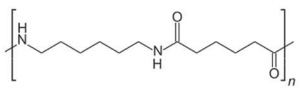	PA66CF
PA12	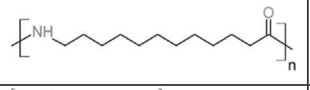	PA12GF
PPA	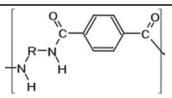	PPATF
PPS	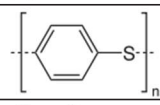	PPSCFGr
PTFE		PTFECFGr PTFEBr
PEEK1 PEEK2 PEEK3	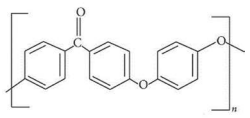	PEEK1TFCFGr PEEK2TFCFGr
PAI	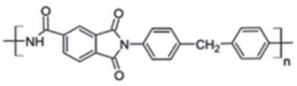	PAITFGr
PI1 PI3	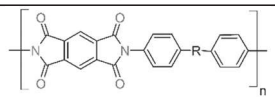	PI3Gr PI3MoS$_2$
PBI	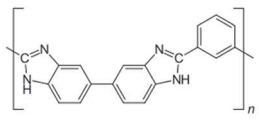	

2.3 Surface analyses

Worn surfaces of the polymer composites and transfer films formed on the disks were inspected by means of an optical microscope (Keyence, VHX-500), 3D profilometer (nanofocus) and a scanning electron microscope (SEM, Zeiss Supra™40) equipped with energy dispersive X-ray spectrometer (Thermo NSS). Chemical analyses were performed by micro-ATR-IR attenuated total reflection (Hyperion 3000, Bruker) with a germanium crystal. The wavelength range was set from 4000 cm^{-1} to 500 cm^{-1}.

3 Results at ambient temperature

3.1 Friction at ambient temperature

Figure 1 shows the average friction coefficient of neat polymers in air and hydrogen at ambient temperature. In general, hydrogen environment has a beneficial effect on the friction behavior of neat polymers. The friction coefficient is significantly reduced for PI (80%) > PA66 (65%) > PAI (60%) > PBI (33%) > TPE (26%) > PA12 (20%) in H_2 but increases of more than 50% for POM. The coefficient of friction of PPA,

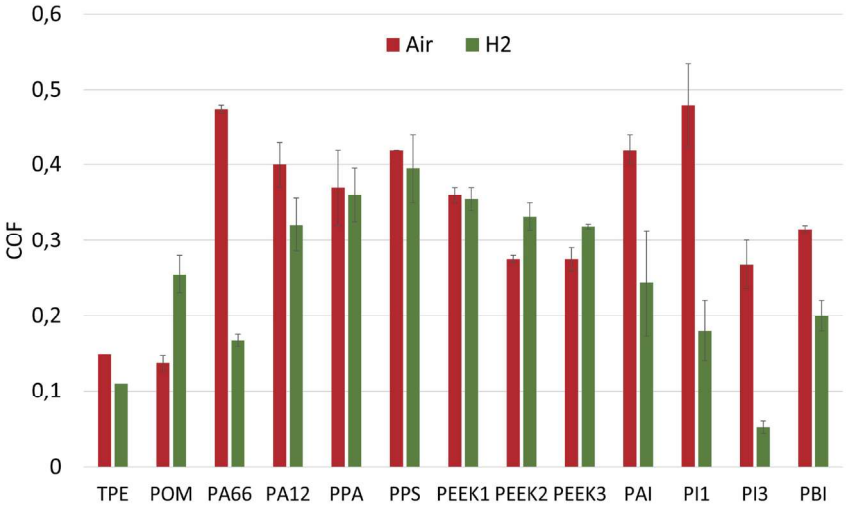

Fig. 1 Friction coefficient of neat polymers at ambient temperature in air and hydrogen

PPS and PEEK1 are less affected by the hydrogen atmosphere. Interestingly, different PEEK grades present slight changes, particularly with regards to the friction coefficient in air. For PI materials with distinct chemical formulation, different friction values are observed both in air and H_2. In these test conditions, the lowest friction coefficient is obtained with PI3 in hydrogen.

In order to verify the influence of the hydrogen compared to dry environment, further tests were performed in vacuum during 2000 m followed by hydrogen for 3000 m. The evolution of the friction coefficients as a function of sliding time in air, vacuum and hydrogen are plotted in Fig. 2 for selected polymers. The friction coefficient of PBI, PAI and PA66 decrease significantly in vacuum and in hydrogen compared to air. For PA66, the introduction of hydrogen after vacuum condition decreases further the friction coefficient (Fig. 2c). Contrarily to PI1 that showed similar friction in vacuum and hydrogen environment against stainless steel disk in [18], the friction curve of PI3 decreases moderately in vacuum compared to air, but suddenly and significantly after introduction of hydrogen (Fig. 2d). After a short running in period, the friction of POM stabilized in air at 0.15, while unstable friction behavior is observed in hydrogen (Fig. 2e), reaching similar value as in vacuum condition.

Figure 3 shows the friction of composite materials in air and hydrogen. The friction is improved in hydrogen for all materials except for PTFE matrix composites. Lower friction coefficient is obtained with PPS and PEEK materials, both containing graphite and CF. Comparing with the value of the neat polymers that have similar friction in air and hydrogen, it is obvious that the fillers have a beneficial effect in hydrogen. Contrarily to ambient air, the addition of CF in PA66 does not lead to a decrease in the COF in hydrogen, since the value of CF filled PA66 is similar to that of neat PA66 in hydrogen. Therefore, it can be concluded that most effects are due to the presence of graphite. As expected, the addition of MoS_2 in PI3 leads to an increase in the COF in air compared to the neat polymer. In hydrogen MoS_2 filled PI3 has a lower friction than in air, but higher than the neat PI3 that shows the lowest friction in this condition.

3.2 Wear at ambient temperature

The specific wear rates of neat polymers are presented in Fig. 4. Lower or similar values are obtained in hydrogen compared to air for most polymers, except for PI3, which has a noticeable higher wear rate. The three types of PEEK have a lower wear rate in hydrogen, while PPS and PPA remain insensitive to the environment. Under these test conditions, PBI has the lowest wear rate in hydrogen among the neat polymers. Overall, hydrogen environment influences more friction than the wear rate.

The specific wear rates of the composites sliding in air and hydrogen are compared in Fig. 5. Best performances are obtained with PPSCFGr, PEEKTFCFGr and PI3Gr, which confirmed the beneficial effect of graphite. The addition of CF in PA66 leads to a reduction of the wear rate compared to the neat polymer regardless of the environment. Adding glass fibers in PA12 reduced the wear rate in air but increased it in hydrogen. Similar effects are seen by adding PTFE in PPA. As for PTFE composites, both materials have the highest wear rate in air and in hydrogen environment, although the value decreases slightly for the graphite and CF containing PTFE in hydrogen. MoS_2 filler has only a small effect on the wear rate of PI3 composite in hydrogen.

3.3 Surface analyses

Surface images of the wear track on the disk after tests at ambient temperature in air and gaseous hydrogen are presented in Figs. 6 and 7. Comparing the morphology of the wear track, most significant differences are observed with PI3, PBI, POM, PA66 and PAI (Fig. 6). As observed in Figs. 6a and 6b, low friction and wear rate of PBI and PI3 are mainly associated with a formation of a homogenous transfer film in hydrogen, while lumpy particles or patchy transfer are seen on the disk after the experiments in air. POM formed a wider track in hydrogen compared to air (Fig. 6c), while the transfer of PA66 and PAI are obviously thicker in hydrogen environment (Figs. 6d and 6e). With PA12, PPA, PEEK and PPS, however, only lumpy transfer is observed in both ambient air and hydrogen gas (Fig. 7).

Images of the worn polymer pins are shown in Fig. 8. The surfaces of PBI and PI show significant abrasive wear in both environments, whereas adhesive wear with polymer back transfer on the pin is observed particularly in air. For POM and PA66, however, the surface of the worn pin is different: abrasive wear is predominant in air and many wear particles are seen on the pin surface of POM after test in hydrogen.

Some surface images of the wear track formed with composite materials and the corresponding worn pins are presented in Fig. 9. For PEEK composite (filled with CF, PTFE

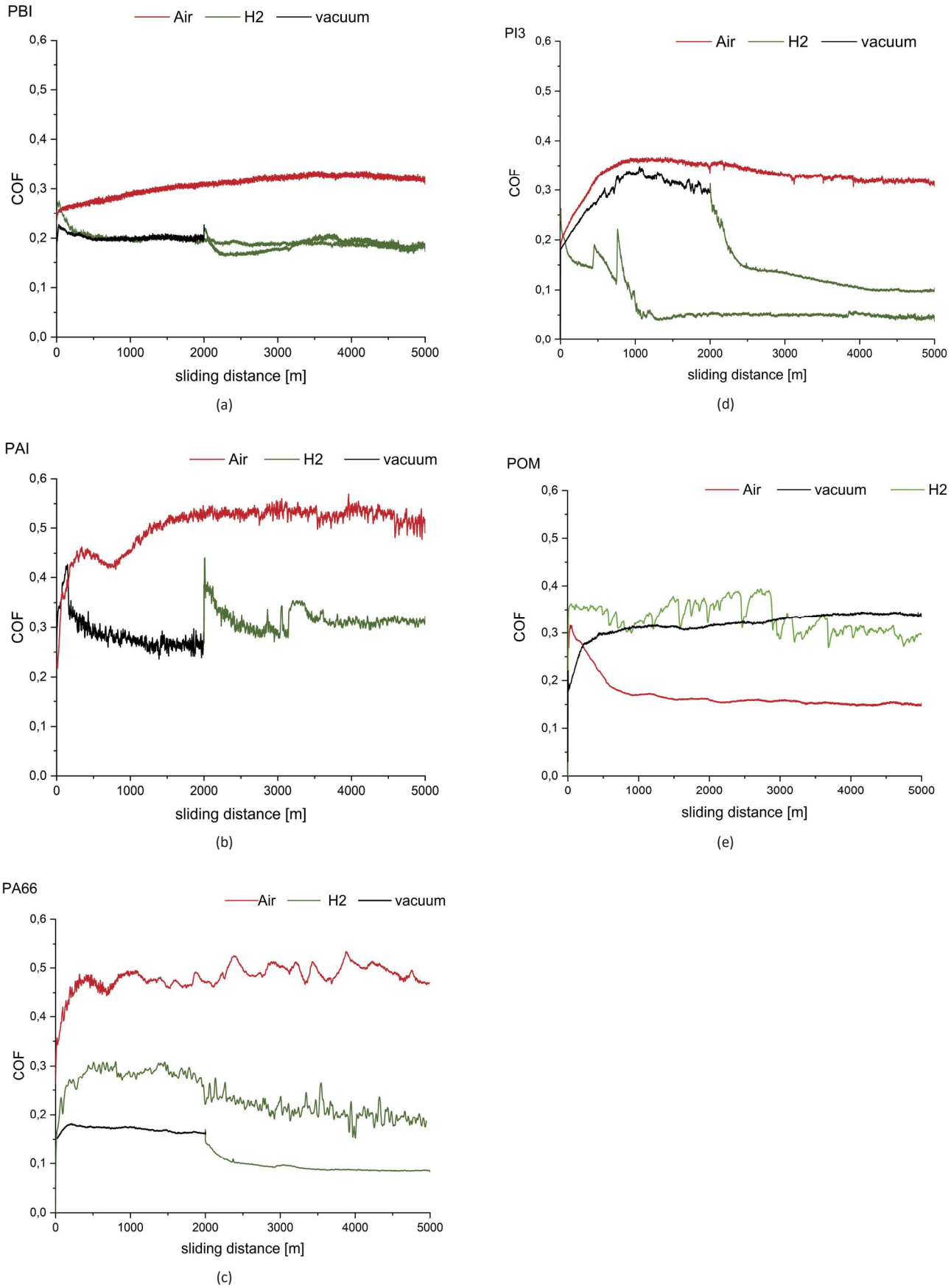

Fig. 2 Friction curves of (a) PBI, (b) PAI, (c) PA66, (d) PI3 and (e) POM against 304 disk in air, vacuum and hydrogen at ambient temperature

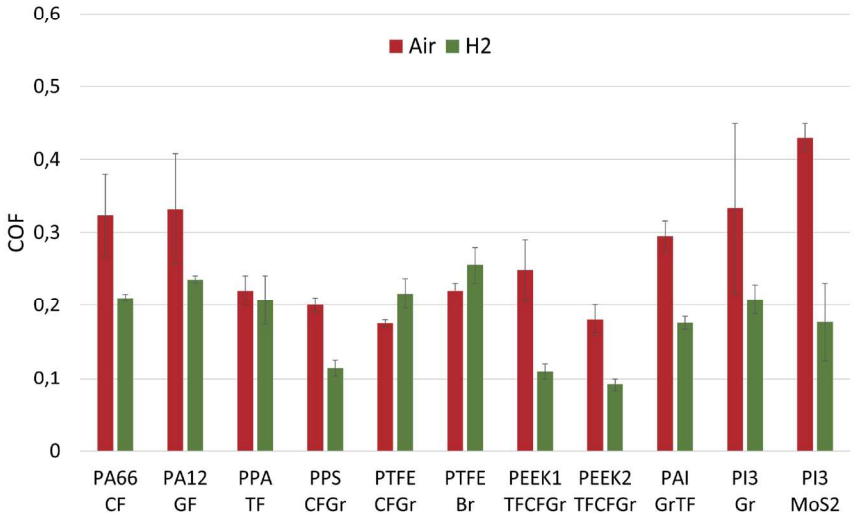

Fig. 3 Friction coefficient of composites in air and hydrogen at ambient temperature

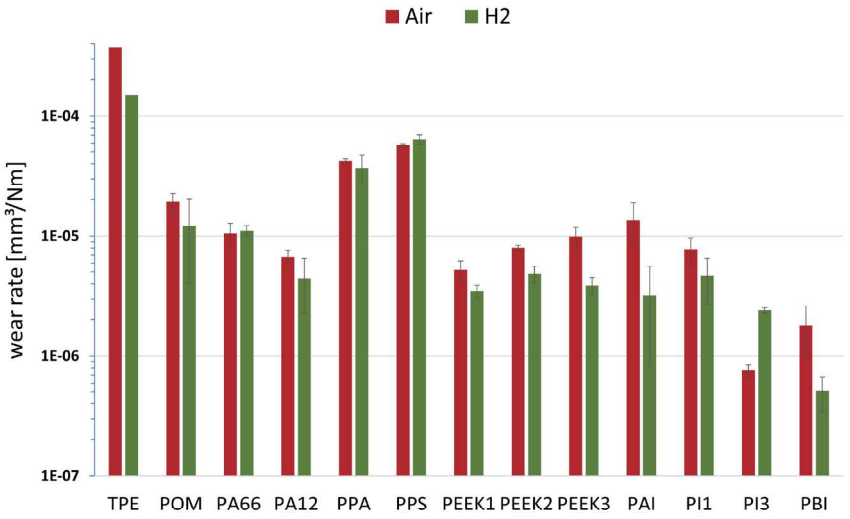

Fig. 4 Wear rate of neat polymers in air and hydrogen at ambient temperature

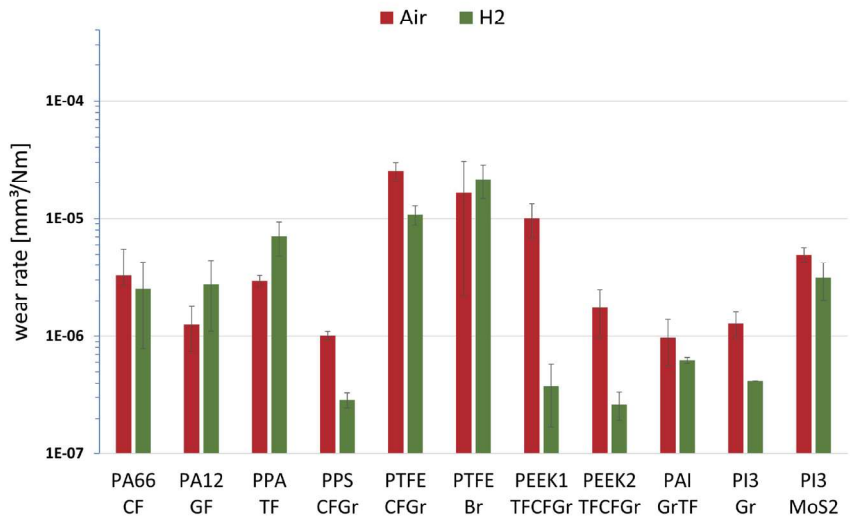

Fig. 5 Wear rate of composites in air and hydrogen at ambient temperature

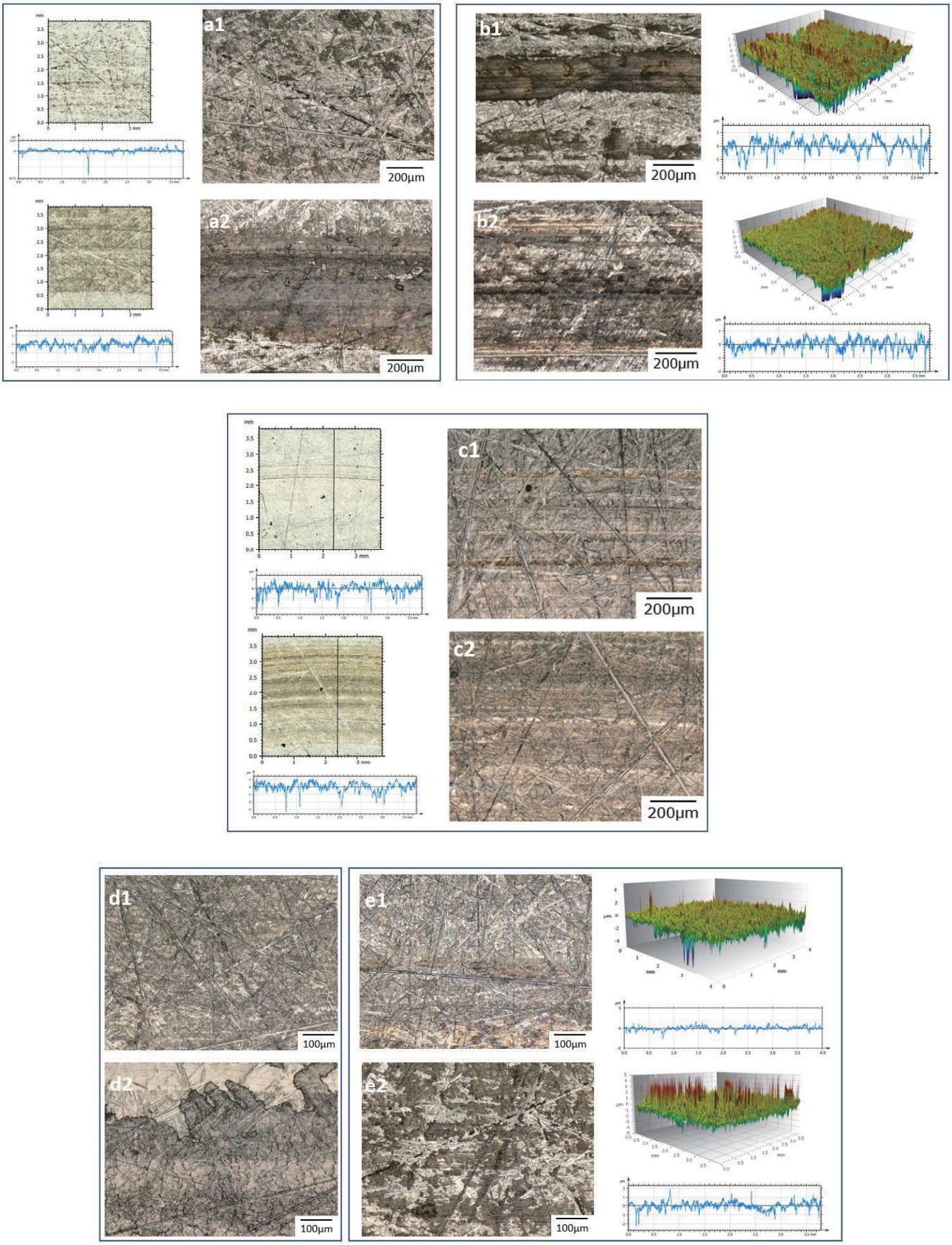

Fig. 6 Wear track after tests against PI3 (a), PBI (b), POM (c), PA66 (d) and PAI (e) in air (1) and gaseous hydrogen (2)

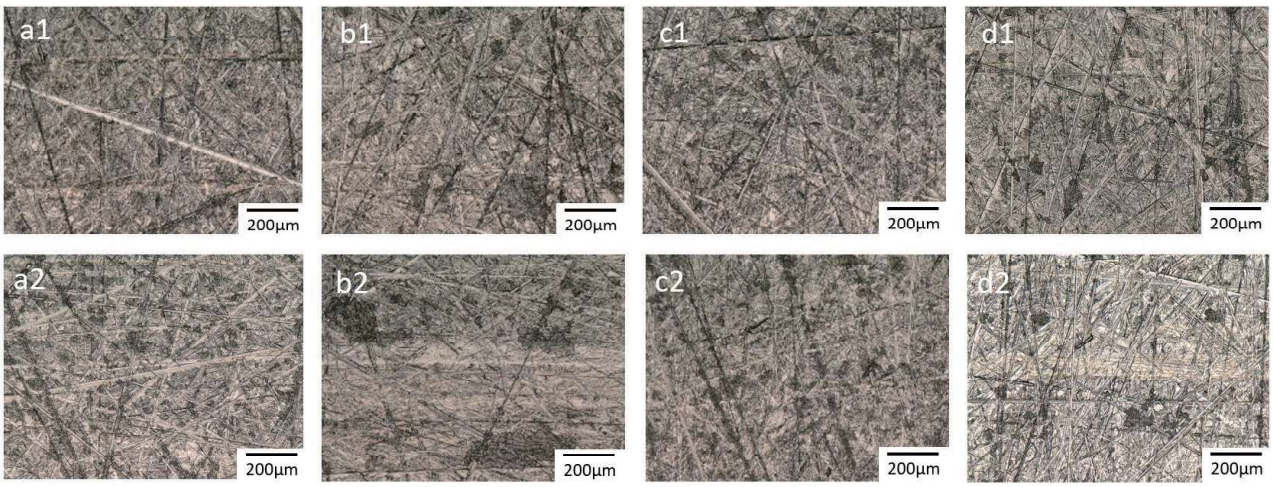

Fig. 7 Wear track after tests against PA12 (a), PPA (b) PEEK2 (c) and PPS (d) in air (1) and gaseous hydrogen (2)

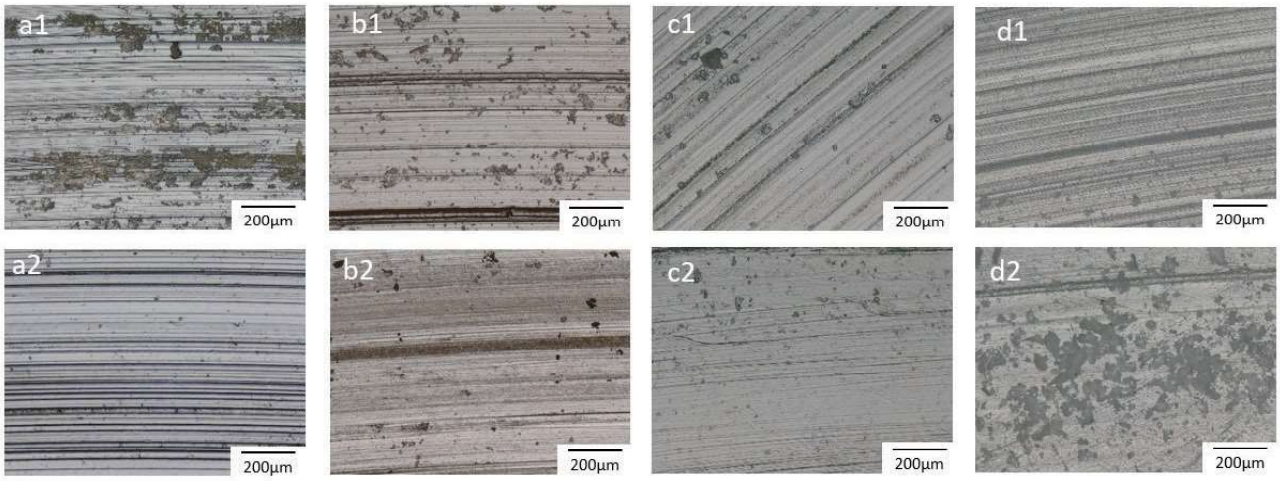

Fig. 8 Images of the worn pin surface of PBI (a), PI3 (b), PA66 (c) and POM (d) after tests in air (1) and gaseous hydrogen (2)

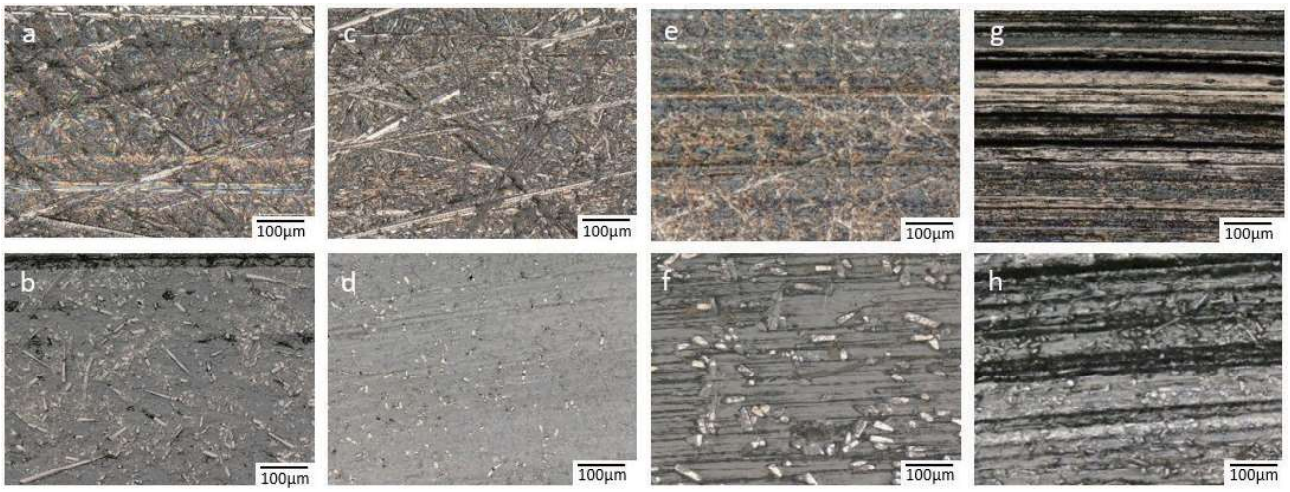

Fig. 9 Images of the wear track of PEEKTFCFGr (a, c) and PA12 GF (e, g) and the worn pin surface PEEKTFCFGr (b, d) and PA12 GF (f, h) after tests in air and gaseous hydrogen, repectively

and graphite) a transfer film is present in both conditions, and the surface of the pin is smooth after sliding in hydrogen environment. On the other hand, the morphology of the glass filled PA indicates strong abrasion after sliding in hydrogen environment.

Infrared spectroscopy was used to characterize the surface of the disks after experiments. Appendix A compares the ATR-IR spectra of PI1 and PI3 after tests against 304 in air and hydrogen. While the spectra of PI1 are identical in air and hydrogen, two new aliphatic absorption bands were detected only after hydrogen environment for PI3.

4 Results at cryogenic temperature

In this section, test results performed in liquid hydrogen are compared with the results in gaseous hydrogen at ambient conditions to evaluate the influence of the temperature.

4.1 Friction in gaseous and liquid hydrogen

The average friction coefficient of neat polymers and composites in gaseous and liquid hydrogen are presented in Figs. 10 and 11. All neat polymers have a lower friction coefficient at cryogenic temperature except PI3, which has the lowest value in gaseous hydrogen. The decrease is particularly pronounced for PA polymers with a COF of 0.07.

The friction coefficient of PA, PPS and PTFE composites decrease in LH_2, but this is not the case for PEEK and PI composites. Comparing to the neat polymer, the addition of GF increases the COF of PA12 in LH_2. Furthermore, adding graphite or MoS_2 does not improve the COF of PI3 in LH_2. Friction curves indicate a rather unstable friction for PA12 and PEEK composites in LH_2, while PTFE and PI composites have a relatively smooth friction in gaseous and liquid hydrogen (Fig. 12).

4.2 Wear in gaseous and liquid hydrogen

The specific wear rates of the neat polymers and composite

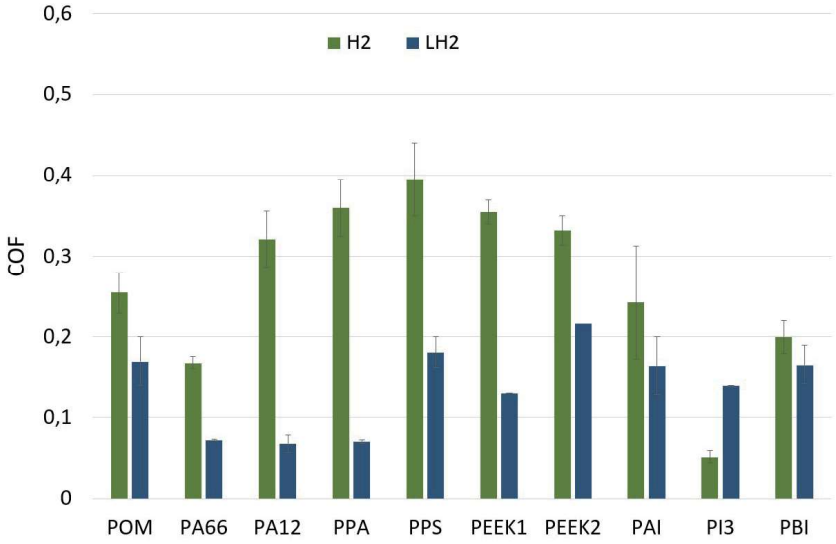

Fig. 10 Friction coefficient of neat polymers in gaseous hydrogen at ambient temperature and in liquid hydrogen

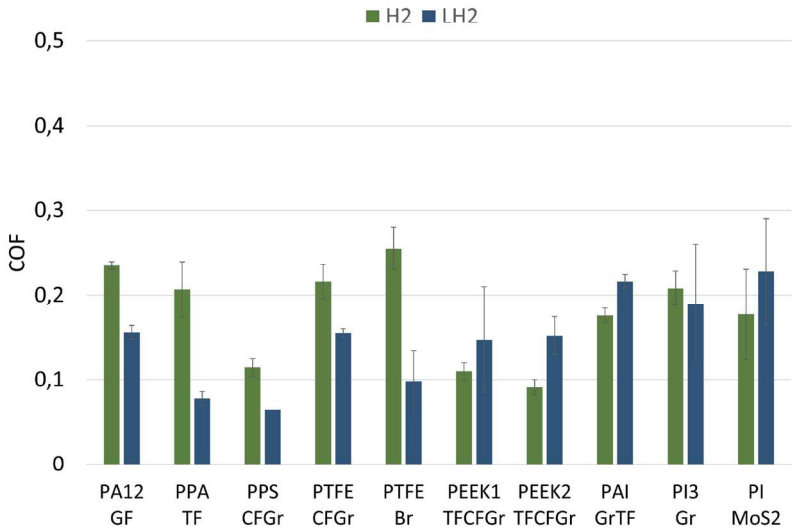

Fig. 11 Friction coefficient of composites in gaseous hydrogen at ambient temperature and in liquid hydrogen

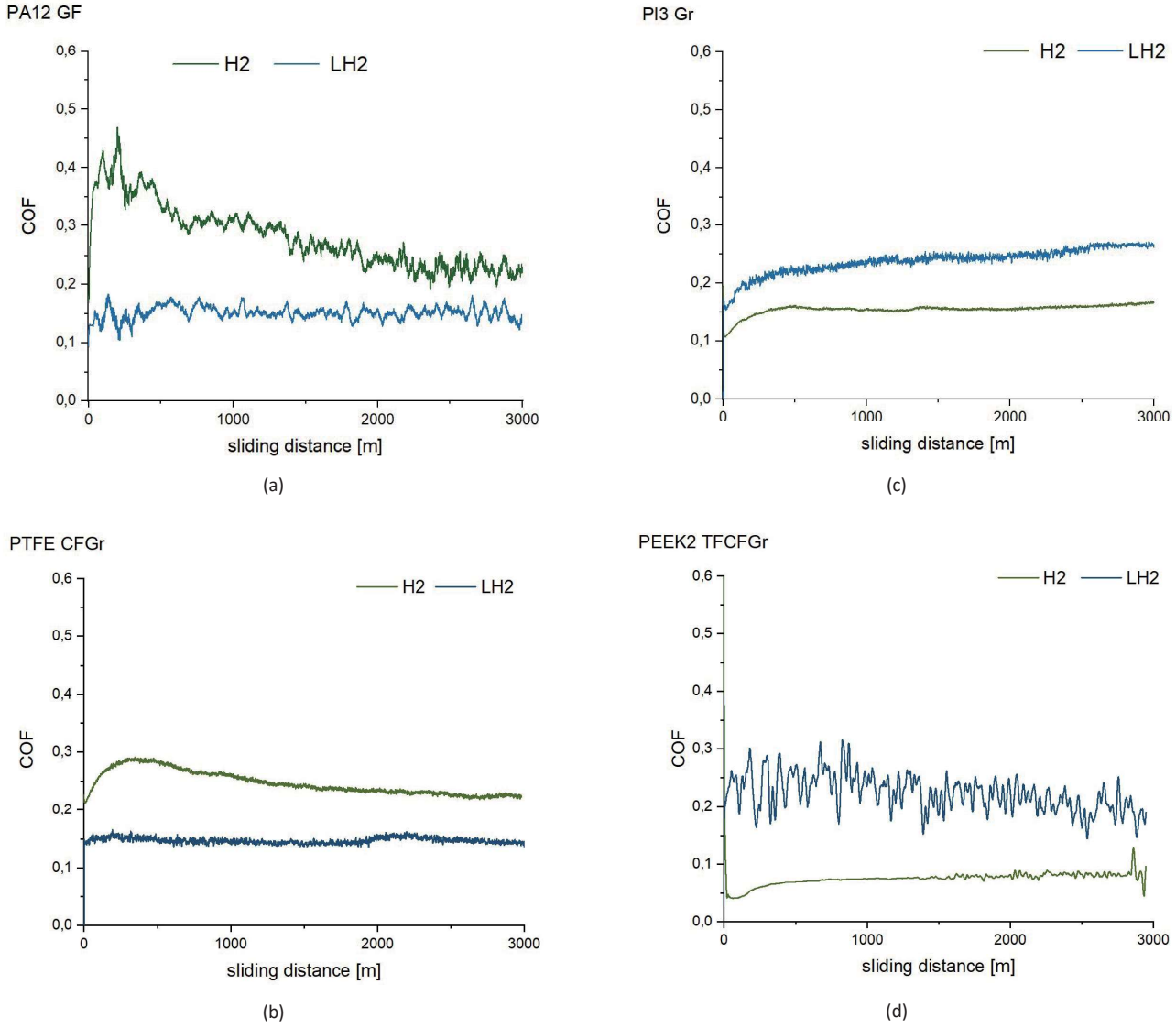

Fig. 12 Friction curves of PA12GF (a), PTFECFGr (b), PI3Gr (c) and PEEKTFCFGr in gaseous hydrogen at ambient temperature and in liquid hydrogen

materials sliding in gaseous and liquid hydrogen are compared in Figs. 13 and 14, respectively. In liquid hydrogen, the average wear values decrease significantly for PA66, PA12, PPA, PPS and PEEK polymers, but remain unchanged for PAI and PI3. While PBI has moderate increased wear in LH_2, the tests with POM had to be stopped after 1000 m in LH_2 due to severe wear.

PA12 and PPA composites have a lower wear rate at cryogenic temperature, but the addition of GF or PTFE, respectively, does not improve the wear resistance comparing to the neat polymer in LH_2. Both PTFE composites show a significant lower wear rate in LH_2. On the contrary, the performance of PEEK composites is worse at cryogenic temperature.

4.3 Surface analyses

Surface images of the wear track and worn pin surface of selected neat polymers after tests in LH_2 are presented in Fig. 15. The transfer film consists of powdery wear debris trapped mechanically on the groove of the disk. For PA66, PA12 and PPS, this produces a thin film covering the wear track. The transfer film observed in gaseous hydrogen with PBI (Fig. 6b2) is friable in liquid hydrogen (Fig. 15h). On the surface of worn pins, mainly abrasive ploughing is observed for PAI, PEEK or PPS, while fatigue wear is predominant for neat PPA in LH_2.

Figure 16 presents the wear track of PEEK, PPS, PI and PTFE composites in gaseous and liquid hydrogen. The transfer film of the PEEK composite is inhomogeneous in LH_2, while a thin transfer is formed at cryogenic temperature for PPS, PTFE and PI composites. EDX analyses of the wear track indicate that the transfer film contains not only a carbon layer but also polymers (Appendix B). The distribution of PTFE in the transfer film is more pronounced than that of PPS, which is mainly trapped in the disk roughness.

Worn polymer surfaces after tests in LH_2 and H_2 at ambient condition are compared in Fig. 17. On the surface of the PA composite, which shows large abrasiveness in gaseous hydrogen, glass fibers remain embedded in the matrix in LH_2. Similarly, CF are presents on the pin surface of PTFE composite in LH_2. On the other hand, fibers are hardly seen on the worn surface of the PEEK composite.

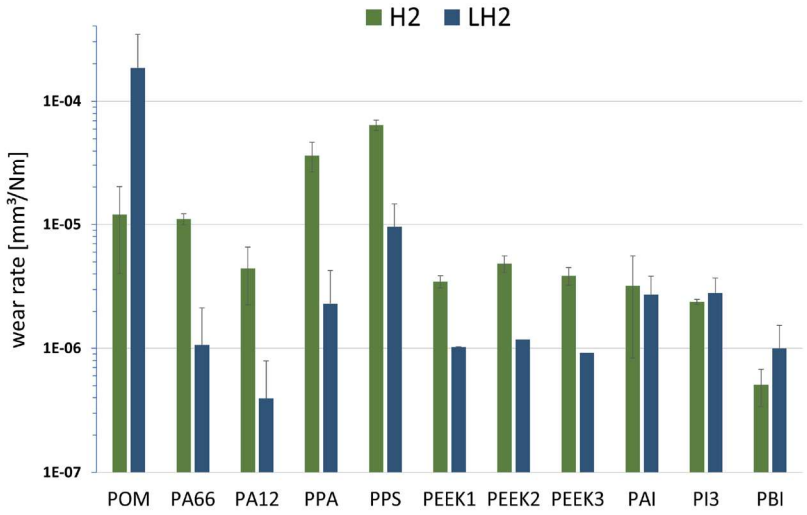

Fig. 13 Wear rate of neat polymers in gaseous hydrogen at ambient temperature and in liquid hydrogen

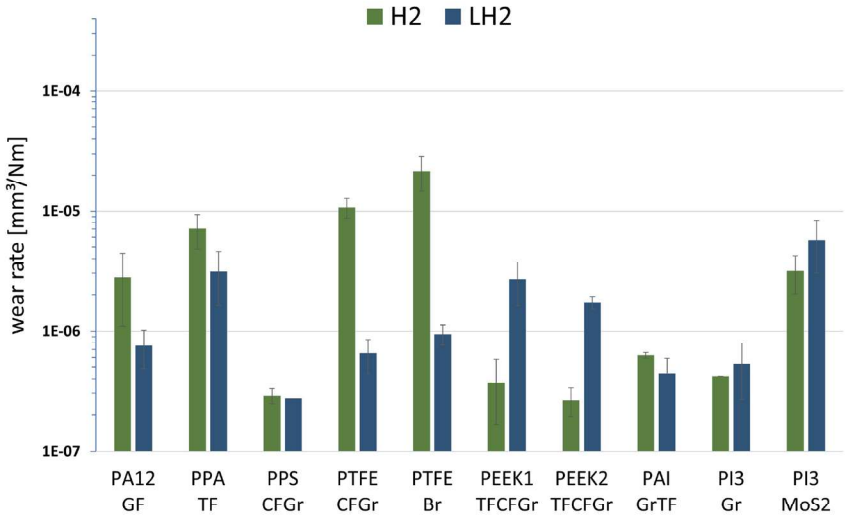

Fig. 14 Wear rate of polymer composites in gaseous hydrogen at ambient temperature and in liquid hydrogen

5 Discussion

The results described above suggest a certain influence of hydrogen environment on the friction and wear behavior of polymer materials. Comparing to moist air, hydrogen provides a better dissipation of heat, an absence of oxygen and the moisture content is less than 5 ppm. Furthermore, hydrogen is chemical active gas that may reduce oxide layers on the counterface and induce tribological reactions. The cooling effect may be effective for some polymers with low heat resistance like TPE. For high performance polymers, however, the formation of a transfer film is often related to the softening of the polymers, that occurs due to frictional heat. As seen in the first section, if hydrogen environment has a beneficial effect on the friction behavior of most neat polymers, significant decrease of the COF was observed for PA66, PAI, PI and PBI. Surface analyses indicated that low friction and wear rate are associated with a formation of transfer film in hydrogen contrary to air. Therefore, the heat dissipation properties of the environment cannot be the main factor to consider, especially since the experiments in vacuum also show lower friction coefficient than in air. This suggests primarily an effect of the dry atmosphere or lack of oxygen.

As described in [16] for PI1, H-bonds between water molecules and the carbonyl groups of PI in moist environment restricts the molecular mobility of polymer, preventing orientation and polymer transfer, which leads to higher friction in moist air. On the contrary, in dry atmosphere, the PI chains are more flexible and can easily be oriented in sliding direction to form a transfer film, reducing friction drastically. For PI1, the friction and wear values were found to be similar in vacuum and hydrogen [18]. Similarly, it is noticeable that the polymers that are the most affected by hydrogen environment are also moisture sensitive [26]. This is the case for PBI, PAI, PA66 and PI. As shown in Fig. 2, the friction of PBI and PAI are similar in vacuum and in hydrogen, suggesting an effect of moisture content. The lack of H-bonds may facilitate the mobility of polymer chains, reducing shear strength and improving film formation. Similarly, for PA polymers, hydrogen bonds are present naturally between the molecules, and the effect of moisture is also well known especially for PA66, which results in abrasive wear in moist air. As seen in Fig. 2, the coefficient

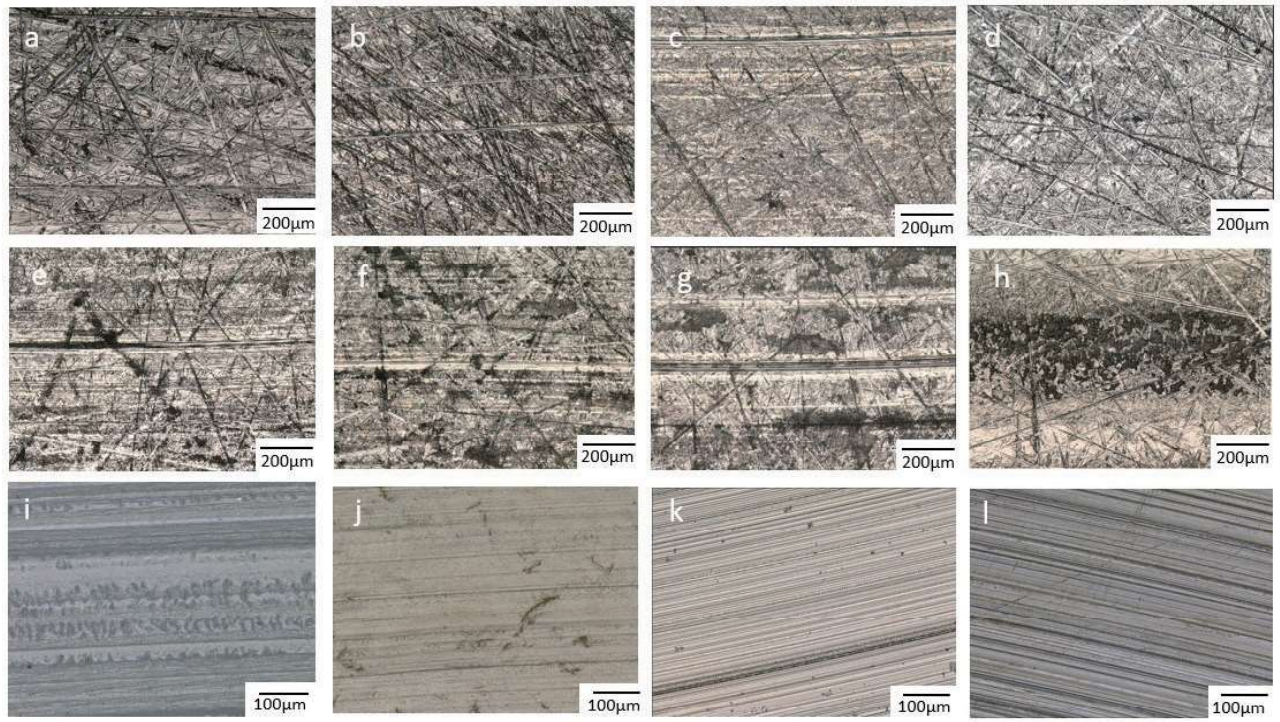

Fig. 15 Images of the wear track after tests against POM (a), PA66 (b), PA12 (c), PPS (d), PPA (e), PEEK1 (f), PEEK3 (g), PBI (h) and images of the worn pin surface of POM (i), PPA (j), PEEK3 (k) and PPS (l) after tests in liquid hydrogen

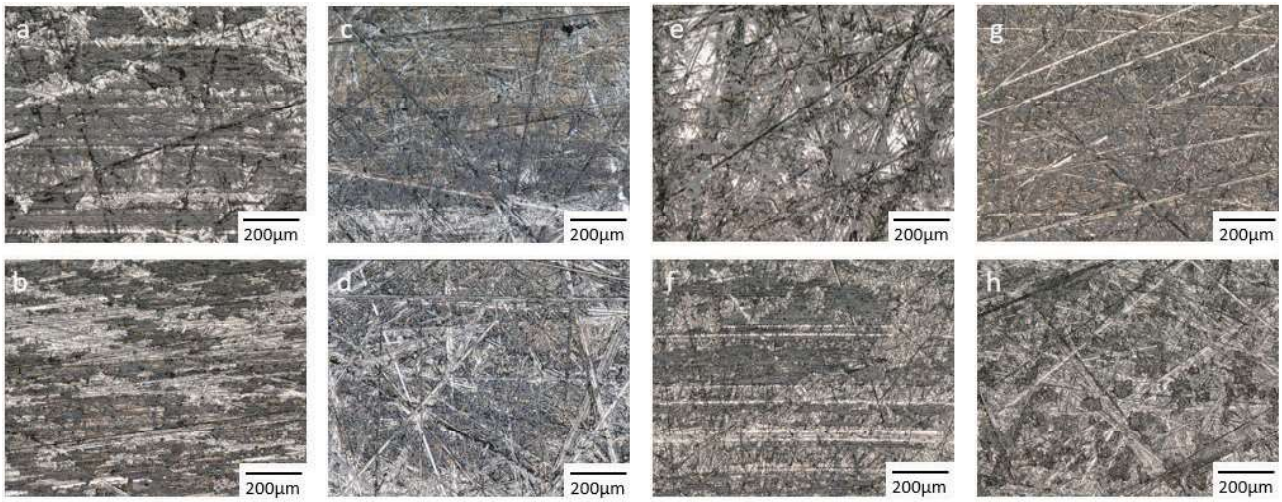

Fig. 16 Images of the wear track of PTFE CFGr (a, b), PPS GrCF (c, d) , PIGr (e, f) and PEEK CFTFGr (g, h) after tests in gaseous and liquid hydrogen, respectively

of friction of PA66 in vacuum is much lower than in air. By comparing with the test performed only in hydrogen, the friction is lower in vacuum during the first 2000 m. In this case, the removal of water molecules in vacuum is more efficient than in hydrogen. After 2000 m in vacuum, the friction decreases rapidly with the introduction of hydrogen in the chamber. This indicates a beneficial effect of hydrogen molecules, possibly by saturation of free radicals.

Contrarily to PI1 that showed similar coefficient of friction in vacuum and hydrogen environment [18], lower values are obtained with PI3 in hydrogen. In fact, according to the supplier, PI3 has a much lower moisture uptake than PI1, which relates the moderate reduction of the friction coefficient in vacuum compared to air. With the introduction of hydrogen gas in the chamber, a sudden decrease in the friction curves emphasizing the effect of H_2 molecules in the friction process. ATR-IR analyses indicate some new peaks arounds at 2850 and 2925 cm^{-1} corresponding to the C-H stretching of saturated hydrocarbons, which possibly act as friction reducer in hydrogen.

Concerning POM, a wider transfer film is present in hydrogen compared to air. The higher friction in hydrogen may be due the fact that the friction between POM and itself is higher than POM against stainless steel (0.4 POM vs POM).

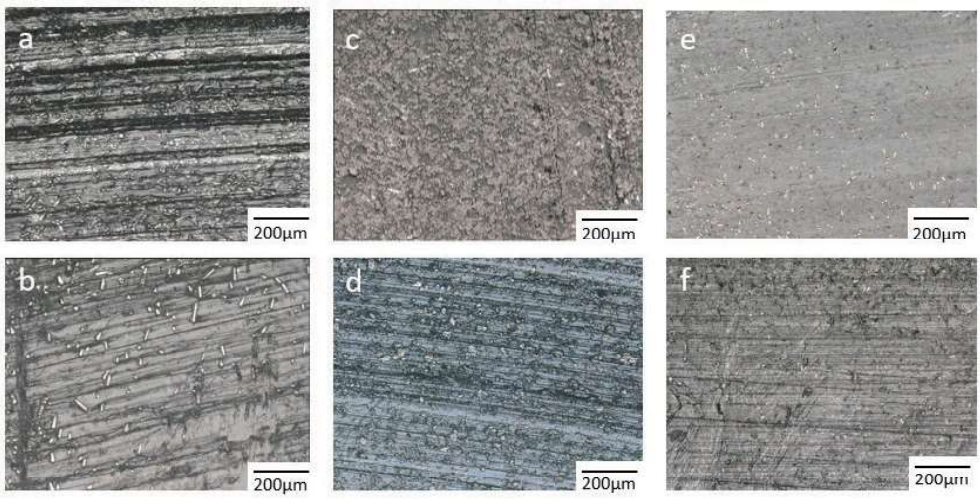

Fig. 17 Surface images of the composites PA12GF (a, b), PTFE CFGr (c, d), PEEK TFCFGr (e, f) after test in gaseous and liquid hydrogen, respectively

This is confirmed by the large amount of back transferred wear debris on the pin surface in hydrogen environment.

The effect of oxygen couldn't be investigated here since comparisons were made either with vacuum or moist air. Oxidative environment and oxide layers can promote adhesion of polymers on metal surface by forming, e.g. complex metal-organic compounds as observed in [27, 28]. These chemical reactions between polymer and metal depend on the counterface composition [18]. This may increase the friction on the one hand but also facilitate the adhesion of the transfer film on the other hand. As observed in [16], the lack of oxide layer may also promote triboreactions with the fresh metal (AISI 52100). In the present study though, more polymer transfer was observed on 304 disk in hydrogen environment with moisture sensitive polymers. Therefore, adhesion of this transfer should be further investigated in dry air.

The film formation in hydrogen, responsible for the low friction coefficient of the polymer mentioned above, protects the pin surface from wearing out, leading to lower wear rate for most polymers. Only PI3, which has the lower wear rate in air, shows increased value in hydrogen. This is possibly due to the formation of saturated hydrocarbon during the friction process that might weaken the polymer. Further analyses should be done to clarify this effect.

Regarding the composites, the addition of fillers and fibers have different effects on friction and wear. As seen in our previous study, lower friction and wear were obtained with graphite filled polymers in hydrogen [17]. It was reported that the lubricating effect of graphite is more effective in hydrogen than in humid air, due to the saturation of the dangling bonds with hydrogen. Similarly, the addition of carbon fibers alone could reduce the friction coefficient of PA66 in hydrogen by forming a carbon rich layer, but the wear rate was not affected as much as for the graphite filled composites. Regarding to GF, a higher wear rate was obtained in hydrogen environment due to high abrasiveness as seen in (Fig. 9). This interaction between glass fibers and hydrogen has been observed in [15], which suggests the removal of protective oxide layer of the disk as a possible reason for high abrasion.

In the second part of the study, tribological experiments were performed with selected materials in liquid hydrogen. Three different behaviors were observed depending on the polymer matrix. First, for most neat polymers, lower friction and wear are obtained at cryogenic temperature, as already observed for neat PEEK in previous work [24]. This is the case of PA66, PA12, PPA, PAI, PEEK and neat PPS. This has been attributed to the increased hardness of the polymer, leading to lower deformation and higher wear resistance. For these polymers, abrasive wear is predominant in LH_2. Powdery wear debris, mechanically trapped on the disk surface, forms a protecting layer. In particular, significant improvements were obtained for PA based polymers, which could form a very thin film in LH_2.

PI and PBI represent a second group of neat polymers with distinct tribological behavior from those described above. For both polymers, which show the best results in gaseous hydrogen, the friction and wear rate, respectively, are higher at cryogenic temperature. In these cases, the transfer film developed in gaseous hydrogen become friable in LH_2. Finally, POM shows a unique behavior as it fails at cryogenic temperature, despite of its high modulus at cryogenic temperature [29]

Concerning the composites, significant improvements are obtained with PTFE matrix, which combines higher hardness and capability to form a transfer film at cryogenic temperature. Also, graphite filled PPS and PI composites that perform the best in gaseous hydrogen have similar wear rate in liquid hydrogen due to the formation of a transfer film. PEEK composites, however, behave differently from the other composites at cryogenic temperature. This may be due to the fact that neat PEEK does not form a transfer film at cryogenic temperature, hindering the formation of a graphite rich transfer film in LH_2.

This study points out that the friction and wear behavior of composites materials is relatively complex in LH_2 due to the change in mechanical properties of the polymers at low temperature, and the formation or removal of the transfer film. Also, only powdery debris or thin transfer film are observed in liquid hydrogen. This suggests that, besides the increased hardness of the material and heat removal from the contact area, LH_2 can also contribute to remove larger wear particles from the wear track. A boundary lubricating system, however, is unlikely due to the low viscosity of LH_2 [20].

6 Conclusion

In this study, the friction and wear rate of a wide range of commercially available polymer materials were evaluated against AISI 304 steel disks in air, vacuum, gaseous and liquid hydrogen.

The first part deals with the effect of hydrogen environment compared to air and vacuum at ambient temperature, the second part focusses on the influence of cryogenic temperature.

- According to the results at ambient condition, it is suggested that the effect of hydrogen environment on the tribological behavior of neat polymers can be related to lack of moisture and H-bonds between the polymer molecules. This is the case for PBI, PI1, PA66 and PAI, whose friction decreases also in vacuum. For these polymers, low friction and wear are associated with the formation of a transfer film due to improved molecular mobility. Further factors affecting the adhesion of the transfer film may still be considered, in particular the removal of oxide layer in hydrogen. Therefore, experiments in dry air should be investigated in a further study. Concerning PPA, PEEK or PPS, that have relative lower moisture uptake, gaseous hydrogen affects moderately their sliding behavior.
- Saturated hydrocarbons in hydrogen contribute to improve further the sliding behavior of neat polymers, as seen for PA66 and PI3. POM presents a unique behavior as its friction significantly increases in gaseous hydrogen.
- For composite materials, the beneficial effect of graphite on the friction and wear of polymers in gaseous hydrogen was confirmed, while glass fibers have a negative effect due to high abrasiveness. The addition of carbon fibers reduces the friction coefficient but not the wear rate.
- In liquid hydrogen, the wear is reduced compared to ambient conditions for most neat polymers due to higher hardness of the polymer. Again, POM is an exception, that failed at cryogenic temperature. The behavior of composites is more complex and influenced by the formation or removal of transfer film.

This study gives an overview of the sliding performance of some commercially available materials in hydrogen and will possibly help in the selection of reliable friction materials for hydrogen technology. Nevertheless, further investigation should be done at cryogenic temperature, notably regarding mechanical properties and long-term behavior in LH_2. Also, new materials and fillers should be considered to optimize the performance of frictionally stressed parts in gaseous and liquid hydrogen.

Acknowledgement

The authors are grateful to Evonik Operations GmbH, Saint Gobain, DuPont™, Ensinger Sintimid GmbH and TU Kaiserslautern, for supplying some materials for this study and to Mr. Berndes, Mr. Heidrich, Mr. Opitz, Mrs. Slachciak, Mrs. Lagleder and Mrs. Hidde for testing and surface analyses.

References

[1] Yamabe J, Nishimura S. Influence of fillers on hydrogen penetration properties and blister fracture of rubber composites for O-ring exposed to high-pressure hydrogen gas. International Journal of Hydrogen Energy. 2009;34(4): 1977-1989.

[2] Fujiwara H, Ono H, Nishimura S. Degradation behavior of acrylonitrile butadiene rubber after cyclic high-pressure hydrogen exposure. International Journal of Hydrogen Energy. 2015;40(4): 2025-2034.

[3] Ono H, Fujiwara H, Onoue K, Nishimura S. Influence of repetitions of the high-pressure hydrogen gas exposure on the internal damage quantity of high-density polyethylene evaluated by transmitted light digital image. International Journal of Hydrogen Energy. 2019;44(41): 23303–23319.

[4] Fujiwara H, Ono H, Onoue K, Nishimura S. High-pressure gaseous hydrogen permeation test method -property of polymeric materials for high-pressure hydrogen devices (1)-. International Journal of Hydrogen Energy. 2020;45(53): 29082-29094.

[5] Fujiwara H, Ono H, Ohyama K, Kasai M, Kaneko F, Nishimura S. Hydrogen permeation under high pressure conditions and the destruction of exposed polyethylene-property of polymeric materials for high-pressure hydrogen devices (2)-. International Journal of Hydrogen Energy. 2021;46(21): 11832-11848.

[6] Castagnet S, Ono H, Benoit G, Fujiwara H, Nishimura S. Swelling measurement during sorption and decompression in a NBR exposed to high-pressure hydrogen. International Journal of Hydrogen Energy. 2017;42(30): 19359-19366.

[7] Simmons KL, Kuang W, Burton SD, Arey BW, Shin Y, Menon NC, Smith DB. H-Mat Hydrogen compatibility of polymers and elastomers. International Journal of Hydrogen Energy. 2021;46(23): 12300-12310.

[8] Zhou C, Zheng J, Gu C, Zhao Y, Liu P. Sealing performance analysis of rubber O-ring in high-pressure gaseous hydrogen based on finite element method. International Journal of Hydrogen Energy. 2017;42(16): 11996-12004.

[9] Zhou C, Chen G, Xiao S, Hua Z, Gu C. Study on fretting behavior of rubber O-ring seal in high-pressure gaseous hydrogen. International Journal of Hydrogen Energy. 2019;44(40): 22569-22575.

[10] Duranty ER, Roosendaal TJ, Pitman SG, Tucker JC, Owsley SL, Suter JD, Alvine KJ. An *in situ* tribometer for measuring friction and wear of polymers in a high pressure hydrogen environment. Rev. Sci. Instrum. 2017;88(9): 095114. https://doi.org/10.1063/1.5001836

[11] Kuang W, Bennett WD, Roosendaal TJ, Arey BW, Dohnalkova A, Petrossian G, Simmons KL. *In situ* friction and wear behavior of rubber materials incorporating various fillers and/or a plasticizer in high-pressure hydrogen. Tribology International. 2021;153: 106627. https://doi.org/10.1016/j.triboint.2020.106627

[12] Sawae Y, Miyakoshi E, Doi S, Watanabe H, Kurono Y, Sugimura J. Friction and wear of bronze filled PTFE and graphite filled PTFE in 40 MPA hydrogen gas. Proceedings of the ASME/STLE 2011 International Joint Tribology Conference. Los Angeles. California USA. 2011: 249-251.

[13] Sawae Y, Fukuda K, Miyakoshi E, Doi S, Watanabe H, Nakashima K, Sugimura J. Tribological characterization of polymeric sealing materials in high pressure hydrogen gas. In STLE/ASME 2010 International Joint Tribology Conference; ASMEDC. 2010: 251-253. https://doi.org/10.1115/IJTC2010-41238

[14] Nakashima K, Morillo C, Kurono Y, Sawae Y, Sugimura J. Wear mechanisms of PTFE in humidified hydrogen gas. In ASME/STLE 2011 Joint Tribology Conference; ASMEDC. 2011: 229-231. https://doi.org/10.1115/IJTC2011-61180

[15] Sawae Y, Morita T, Takeda K, Onitsuka S, Kaneuti J, Yamaguchi T, Sugimura J. Friction and wear of PTFE composites with different filler in high purity hydrogen gas. Tribology International. 2021;157: 106884.

[16] Theiler G, Gradt T. Tribological characteristics of polyimide composites in hydrogen environment. Tribology International. 2015;92: 162-171.

https://doi.org/10.1016/j.triboint.2015.06.001
[17] Theiler G, Gradt T. Environmental effects on the sliding behaviour of PEEK composites. Wear. 2016;368-369: 278-286. https://doi.org/10.1016/j.wear.2016.09.019
[18] Theiler G, Gradt T. Influence of counterface and environment on the tribological behaviour of polymer materials. Polymer Testing. 2021;93: 106912.
[19] Wisander DW, Ludwig LP, Johnson RL. Wear and friction of various polymer laminates in liquid nitrogen and in liquid hydrogen. Nasa Technical Report. 1966.
[20] Theiler G. PTFE- and PEEK-matrix composites for tribological applications at cryogenic temperatures and in hydrogen. PhD-Thesis- BAM-Dissertationsreihe. Band 14. Berlin. 2005.
[21] Friedrich K, Theiler G, Klein P. Polymer composites for tribological applications in a range between liquid helium and room temperature. In: Sinha SK, Briscoe BJ, Editors. Polymer Tribology. London: Imperial College Press. 2008: 375-413.
[22] Zhang Z, Klein P, Theiler G, Hübner W. Sliding wear of polymer composites in liquid hydrogen media. J Mater. Sci. 2004;39(9): 2989-2995.
[23] Theiler G, Gradt T. Polymer composites for tribological applications in hydrogen environment. In: Proc. 2nd int. conf. on hydrogen safety. San Sebastian. Spain. 2007: 11-13.
[24] Theiler G, Gradt T. Friction and wear behaviour of polymers in liquid hydrogen. Cryogenics. 2018;93: 1-6.
[25] Gradt T, Börner H, Schneider T. Low temperature Tribometers and the behaviour of ADLC coatings in cryogenic environment. Tribology International. 2001;34(4): 225-230.
[26] Baur E, Osswald TA, Rudolph N. Plastics handbook[J]. Hanser Publications. Munich. 2019;10: 9781569905609.
[27] Jintang G, Shaolan M, Jinzhu L, Dapeng F. Tribochemical effects of some polymers/stainless steel. Wear. 1997;212: 238-243.
[28] Burkstrand JM. Metal-polymer interfaces: adhesion and X-ray photo emission studies. J. Appl. Phy. 1981;52: 4795-4800.
[29] Hartwig G. Polymer properties at room and cryogenic temperatures. New York. Plenum Press. 1994.

Appendix

Appendix A : ATR-IR spectra of PI1 and PI3 transfer film against 304 in air and in hydrogen

Figures A1 and A2 compare the ATR-IR spectra of PI1 and PI3 after tests against 304 in air and hydrogen. Both polymers exhibit characteristic imide peaks at 1780 cm^{-1} (C=O symmetric

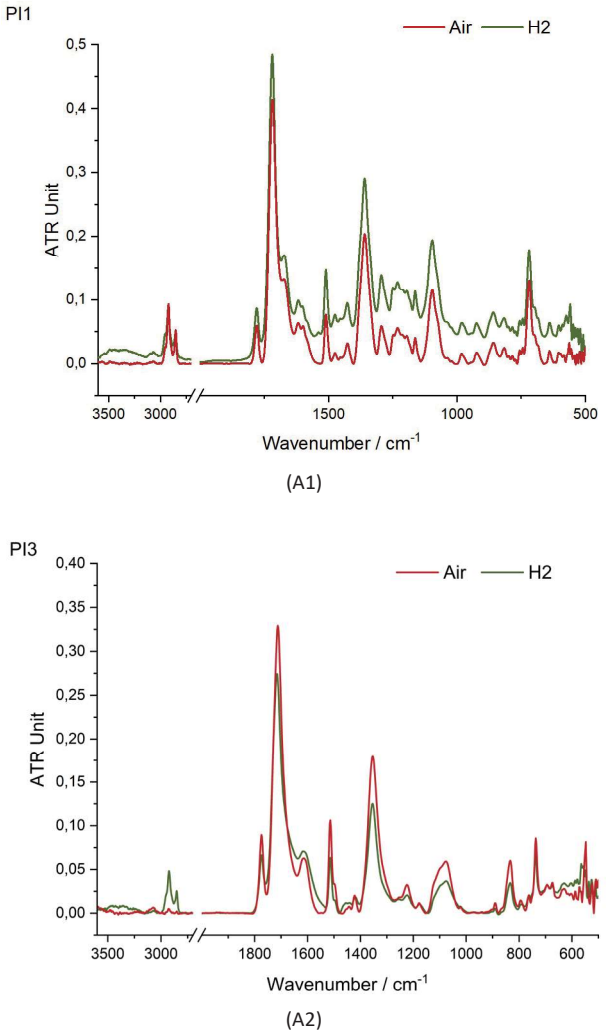

Fig. A ATR-IR spectra of PI1 (A1) and PI3 (A2) transfer film against 304 in air and in hydrogen

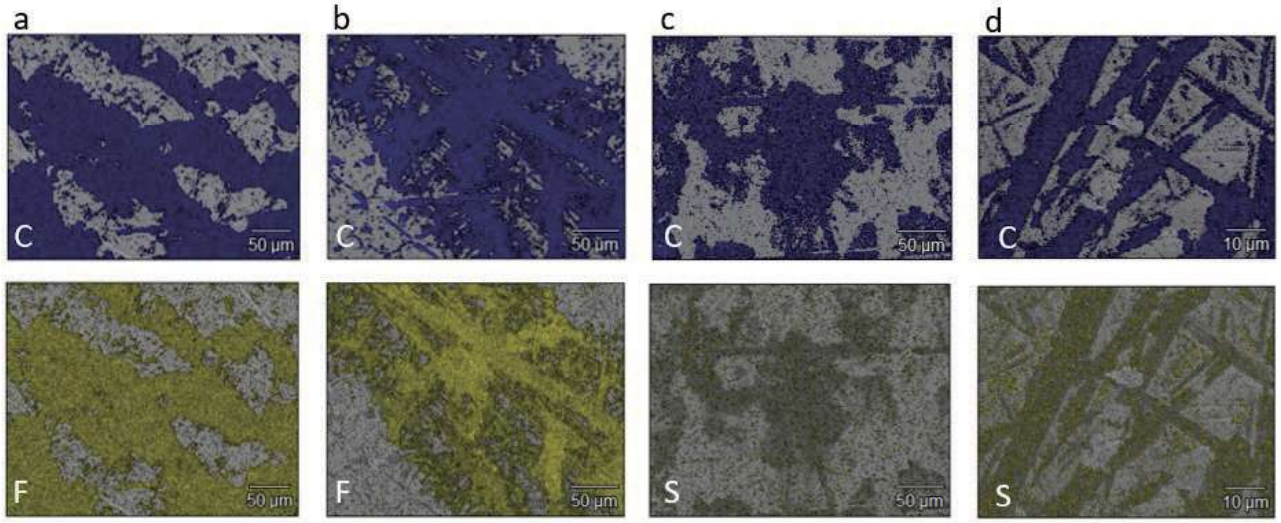

Fig. B EDX analyses of the track of PTFE (a, b) and PPS (c, d) composites after tests in gaseous and liquid hydrogen

stretching) and 1719 cm^{-1} (imide carbonyl C=O asymmetric stretching) that arise from carbonyl stretching in the imide ring. Further peaks at 1360 cm^{-1} and 1100 cm^{-1} are related to C–N and C–N–C stretching, and 720 cm^{-1} to C=O bending. Contrary to PI3, PI1 is characterized by a shoulder at 1670 cm^{-1} that represents the benzophenone carbonyl group in BTDA, and two further absorption bands at 2850 cm^{-1} and 2925 cm^{-1} associated with the aliphatic C-H in CH_2 and CH_3. The spectra of PI1 are identical in air and hydrogen, whereas two new aliphatic absorption bands were detected only after hydrogen environment for PI3.

Appendix B : EDX analyses of the track of PTFE and PPS composites after tests in gaseous and liquid hydrogen

Figure B presents some EDX analyses of the wear track of PTFE (a, b) and PPS (c, d) composites after tests in gaseous and liquid hydrogen, respectively. In both conditions, the transfer film contains C and F or C and S for PTFE and PPS composites, respectively. The distribution of PTFE in the transfer film is more pronounced than that of PPS, which is mainly trapped in the disk roughness.